INL/CON-13-30690
PREPRINT

Stability Study of the RERTR Fuel Microstructure

RRFM 2014

J. Gan
D. D. Keiser, Jr.
B. D. Miller
D. Wachs

April 2014

STABILITY STUDY OF THE RERTR FUEL MICROSTRUCTURE

J. GAN; D. D. KEISER, JR.; B. D. MILLER AND D. WACHS
Nuclear Fuels and Materials Division, Idaho National Laboratory
P. O. Box 1625, Idaho Falls, ID 83415, USA

M. KIRK
Materials Science Division, Argonne National Laboratory
9700 South Cass Ave.,, Argonne, IL 60439, USA

ABSTRACT

The irradiation stability of the interaction phases at the interface of fuel and Al alloy matrix as well as the stability of the fission gas bubble superlattice is believed to be very important to the U-Mo fuel performance. In this paper the recent result from TEM characterization of Kr ion irradiated U-10Mo-5Zr alloy will be discussed. The focus will be on the phase stability of Mo_2Zr, a dominant second phase developed at the interface of U-10Mo and the Zr barrier in a monolithic fuel plate from fuel fabrication. The Kr ion irradiations were conducted at a temperature of 200 °C to an ion fluence of 2.0E+16 ions/cm^2. To investigate the thermal stability of the fission gas bubble superlattice, a key microstructural feature in both irradiated dispersion U-7Mo fuel and monolithic U-10Mo fuel, a FIB-TEM sample of the irradiated U-10Mo fuel (3.53E+21 fission/cm^3) was used for a TEM in-situ heating experiment. The preliminary result showed extraordinary thermal stability of the fission gas bubble superlattice. The implication of the TEM observation from these two experiments on the fuel microstructural evolution under irradiation will be discussed.

1. Introduction

The most popular fuel design for the research and test reactors is the plate type of fuels either in dispersion or monolithic configuration sandwiched with aluminum alloy Al 6061 cladding on both sides. The advantage for a monolithic fuel plate is its higher uranium loading capacity compared to a dispersion fuel. To mitigate the undesired strong interaction between the U-Mo fuel and the Al 6061 cladding, a Zr thin foil of ~ 25 μm is added as a diffusion barrier between the U-Mo and Al 6061. It was found that the Zr foil also develops reaction product at both interfaces of U-Mo/Zr and Zr/Al 6061 from the fuel plate fabrication process [1]. A comprehensive microstructural characterization is required to investigate the radiation stabilities of the relevant interaction product phases at the fuel/cladding interface.

While neutron irradiation and the PIE is an essential part of a fuel development program, ion irradiation, with focus on certain aspect of a fuel material property, is very useful and complementary due to its cost effectiveness, quick turn-around cycle, well controlled irradiation conditions and negligible radioactivity of the sample. The previous ion irradiation study on the stability of interaction product phases at the U-Mo/Al-Si interface provided useful information [2,3]. The Mo_2Zr phase has been identified as a major interaction product developed at the U-Mo/Zr interface [4] or in the U-10Mo-χZr ternary alloy (χ = 1 to 6) [5]. In the open literature, the common crystalline structure for Mo_2Zr is $MgCu_2$ type (cF24, a_0 = 0.75875 nm) as listed in U-Mo-Zr ternary or Mo-Zr binary system phase diagrams [6]. There is also a less common structure for Mo_2Zr phase that is bcc type (cI2, with a_0 = 0.3185 nm) found in a two-phase Mo_2Zr compound where both bcc and $MgCu_2$ type structure co-exist [7,8]. The work by Osten shows that single phase Mo_2Zr in bcc structure cannot be obtained without an extremely fast quenching of 10^5 K/sec following the arc melt [9]. The objective of this work is to investigate radiation stability of the Mo_2Zr phase as an interaction product. This work focuses on microstructure of the Mo_2Zr phase under Kr ion irradiation recorded in-situ along with more detailed post-irradiation TEM characterization.

Equally important to the radiation stability of interaction phase is the stability of fission gas bubble superlattice (GBS) in the U-Mo fuel. GBS is one of the most important microstructural features in the irradiated U-Mo fuel and its radiation and thermal stability may have a strong impact on the fuel performance. Although U-Mo fuel plate operation temperature is limited to below 250 °C due to corrosion of Al alloy cladding, the microstructural stability of U-Mo fuel itself is more or less controlled by the γ-phase stability. There is a great interest of investigating the thermal stability of the GBS in reference to its γ-phase stability. The thermal annealing study on the GBS in the irradiated fuel may be helpful to a better understanding of the U-Mo fuel performance as well as its potential to be used as an alternative fuel for other types of reactors.

2. Experiment

To investigate the radiation stability of the Mo_2Zr interaction phase, a U-10Mo-5Zr alloy was cast via arc melting followed by heat treatments relevant to the fuel fabrication process to produce Mo_2Zr phase for ion irradiation experiment. The cast material was first homogenized at 900 °C for 168 hours and water quenched. The following heat treatment was performed at 650 °C for 3 hours plus water quench which is relevant to the hot rolling process in fuel fabrication. The final step of heat treatment was carried out at 560 °C for 90 min followed by air cool which is representative to the process of hot isostatic press (HIP) as a last step of fuel fabrication. Scanning electron microscopy analysis and X-ray diffraction analysis were performed to confirm the presence of Mo_2Zr phase in the U-10Mo-5Zr alloy. Standard 3.0 mm samples for transmission electron microscopy (TEM) analysis were prepared through slicing, mechanical polishing, disc punching and fine polishing followed by electrical jet polishing to produce thin areas transparent to 200 keV electron beam.

The TEM samples were irradiated with 500 or 250 keV Kr ions at 200 °C to ion doses up to 2×10^{16} ions/cm^2 using the Intermediate Voltage Electron Microscope (IVEM) equipped with a tandem accelerator at Argonne National Laboratory. For 500 keV Kr ions, this corresponds to a peak displacement damage of ~ 145 displacements per atom (dpa) in Mo_2Zr (~ 100 nm thick) estimated from the SRIM calculation [10]. The specimen chamber vacuum is approximately 1.1×10^{-5} Pa (8.0×10^{-8} torr) during ion irradiation. The estimated local temperature uncertainty is approximately ±10 °C. With the selected ion energy of 500 keV or 250 keV, the retention of the injected Kr ions in the electron transparent area (~ 100 nm thickness) of the TEM foil were estimated to be 33% and 95%, respectively. The in-situ TEM analysis was performed using a Hitachi H-9000NAR transmission electron microscope operating at 300 keV during the Kr ion irradiation. Detailed post-irradiation examination (PIE) was performed using a 200 keV JEOL 2010 TEM/STEM system equipped with a LaB_6 filament, a Gatan UltraSacn-1000 digital camera for imaging and a Brukers Si drift detector for composition analysis with Energy Dispersive Spectroscopy (EDS). The TEM selected area diffraction (SAD) patterns from the major zones were used for structural analysis. A Java-version Electron Microscopy Simulation (JEMS) software developed by Stadelmann was used to assist in identifying the phase and indexing the diffraction patterns [11].

Thermal stability study of the GBS was conducted using a Gatan double-tilt TEM heating holder for an irradiated U-10Mo FIB-TEM sample (T_{irr} ~ 140°C, 3.5×10^{21} fissions/cm^3). The GBS microstructure is monitored in-situ during the heating experiment. The temperature ramp rate was approximately 10°C/min where the temperature readout was based on the thermocouple spot-welded at the miniature furnace of the heating holder. The heating holder temperature was raised from room temperature to 700 °C in about 90 min, then kept at ~700 °C for about 30 min, continued to ~850 °C with a reduced rate of ~ 5 °C/min. GBS images at zone [110] were recorded at various points of the heating experiment for evaluation on its thermal stability.

3. Results and Discussion

3.1 Kr ion irradiation stability of Mo_2Zr phase

The alloy matrix remains the bcc structure of U-Mo in γ phase. A low magnification scanning-TEM (STEM) image of the U-10M-5Zr alloy general microstructure is shown in Figure 1 where all precipitates shown in the picture were identified to be Mo_2Zr phase. TEM diffraction analysis of the Mo_2Zr phase in the unirradiated sample confirmed the $MgCu_2$ type structure for Mo_2Zr phase in U-10Mo-5Zr alloy.

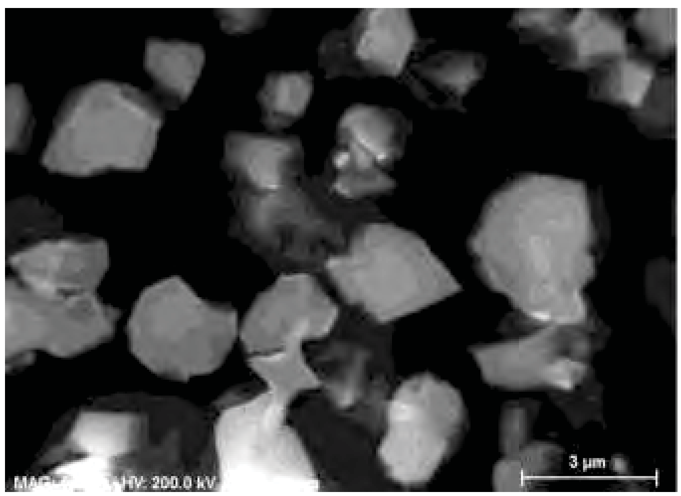

Figure 1. STEM overview image of U-10Mo-5Zr alloy showing Mo_2Zr phase (light contrast).

The microstructural evolution as a function of dose in Mo_2Zr phase under 500 keV Kr ion irradiation is shown in Figure 2. Low-magnification TEM overview images on the top reveal the microstructural change before and after Kr ion irradiation in the Mo_2Zr phase. Six high-magnification TEM images from the same area show the details of the microstructural development as a function of dose. The initial unirradiated microstructure contains a twin and its visibility dropped significantly at a low dose of 1×10^{14} ions/cm^2 and disappeared before the ion fluence of 5×10^{14} ions/cm^2. Significant dislocation development can be seen even at dose as low as 4×10^{13} ions/cm^2. At an ion does of 5×10^{14} ions/cm^2, the development of dislocation as a result of irradiation appears saturated with no significant change up to the final fluence of 2×10^{16} ions/cm^2. A high-resolution image in Figure 3 shows the details of the dislocation tangles and network at the final dose within the same Mo_2Zr precipitate shown in Figure 2. TEM imaging with under- and over-focus conditions at high magnification during both in-situ irradiation and PIE work could not reveal any bubbles in the 500 keV Kr ion irradiated Mo_2Zr phase. It appears Mo_2Zr is quite resistant to Kr ion radiation damage in terms of bubble formation.

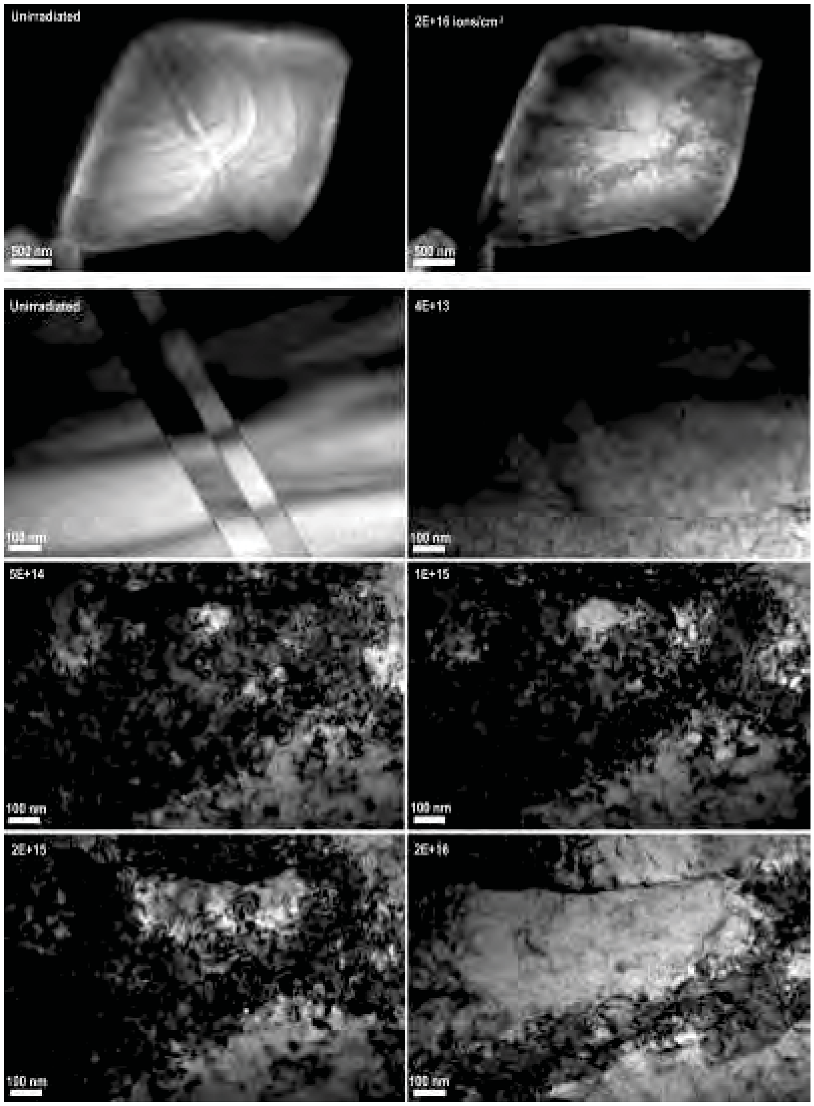

Figure 2. TEM images showing microstructure evolution from the same area in Mo_2Zr.

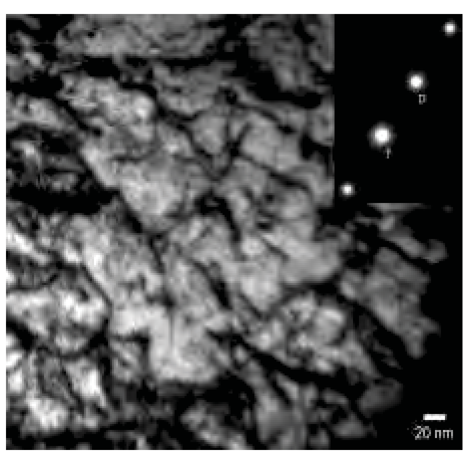

Figure 3. High resolution TEM image showing dislocation tangles and network imaged under g=0-11 from the same area in Figure 2 in bcc Mo_2Zr irradiated to 2×10^{16} ions/cm^2.

The most important finding from the PIE with detailed TEM microstructural characterization is the structural change of Mo_2Zr phase as a result of Kr ion irradiation. The TEM SAD patterns from three major zones ([001], [111] and [101]) for the Mo_2Zr phase in the unirradiated condition in comparison to that of the irradiated condition (2×10^{16} ions/cm^2) are shown in Figure 4. Although the SAD patterns of zone [001] and [111] between the two structures look similar, the corresponding indices are quite different between the two structures. For the irradiated Mo_2Zr, the missing of the original [101] zone pattern shown in the $MgCu_2$ type structure for the unirradiated Mo_2Zr plus the presence of zone patterns from a much smaller cubic structure such as zone [101] confirms the radiation induced structural change.

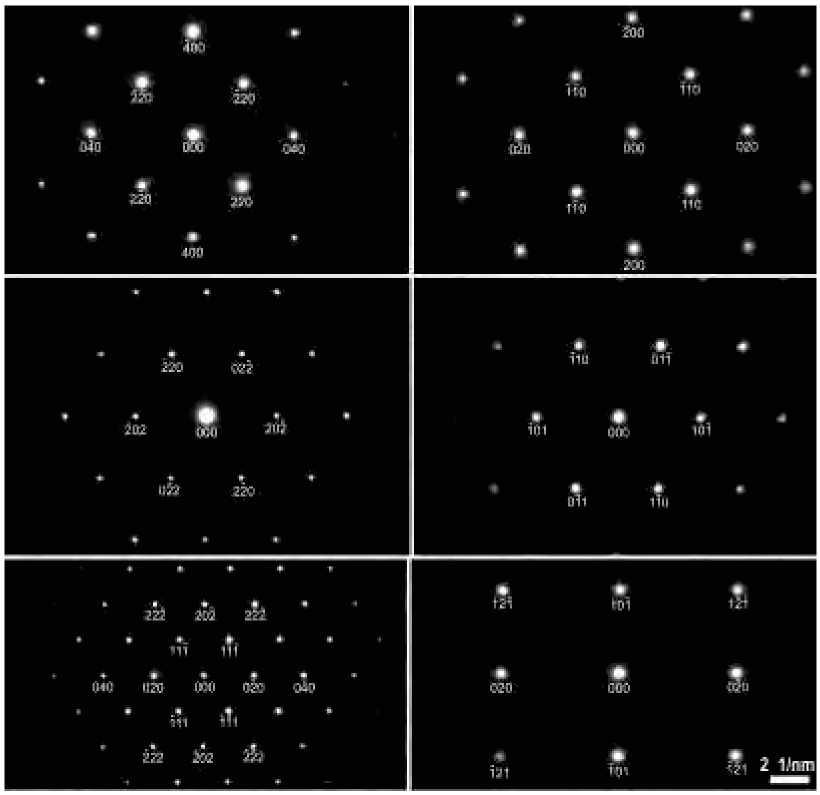

Figure 4. Comparison of SAD zone patterns in Mo_2Zr for unirradiated ($MgCu_2$ type, left) and irradiated to 2×10^{16} ions/cm^2 (bcc, right) at zone [001] (top), [111] (middle) and [101] (bottom).

The $MgCu_2$ type large cubic (a_0 = 0.7588 nm, containing 24 atoms) in the unirradiated Mo_2Zr has changed to the bcc type small cubic (a_0 = 0.3185 nm, containing 2 atoms) in the irradiated condition (2×10^{16} ions/cm^2). The associated volume contraction is estimated to be 11.3%. Unfortunately the exact irradiation doses where the structural transformation was occurring could not be identified in this work without additional Kr ion irradiation experiment using the IVEM due to limited availability for the facility. The transformed Mo_2Zr structure in bcc has a lattice constant similar to that for bcc molybdenum (a_0 = 0.315 nm). Recall that the single phase Mo_2Zr in bcc structure could not be obtained without an extremely fast quenching of 10^5 K/sec following the arc melt [9], the radiation-induced structural transformation for Mo_2Zr phase demonstrated that ion irradiation can lead to a microstructural change far from its thermodynamically stable state. Comparing to the previous work on Kr ion irradiation of U-Mo/Al-Si interaction products [2,3] and disregarding the structural change, the Mo_2Zr phase displayed exceptional radiation tolerance with clear SAD pattern and Kikuchi line pattern at even higher dose. Although the threshold ion dose for the structural transformation was not identified, it is speculated that the threshold dose may be rather low therefore most part of the Kr irradiation was on Mo_2Zr phase with bcc structure which is known for its relative high resistance to swelling and bubble formation comparing to the initial more complex crystalline structure.

One of the objectives for this work is to investigate the bubble development and swelling behavior of the Mo_2Zr phase under Kr ion irradiation relevant to the U-10Mo/Zr/Al-6061 monolithic fuel plate. Since 500 keV Kr ion irradiation to 2×10^{16} ions/cm^2 was ineffective to introduce bubbles in Mo_2Zr phase, it demonstrated the high resistance to bubble formation. In order to develop bubbles under more aggressive condition, the ion energy was reduced to 250 keV to trap more Kr ions in the sample. The amount of Kr ions retained in Mo_2Zr was almost tripled with the reduced ion energy to the same ion fluence. Figure 5 shows the high concentration of small Kr ion bubbles in Mo_2Zr imaged with under- and over-focus conditions for the 250 keV Kr ion irradiation to 2×10^{16} ions/cm^2. The estimated bubble size is approximately ~ 2 nm.

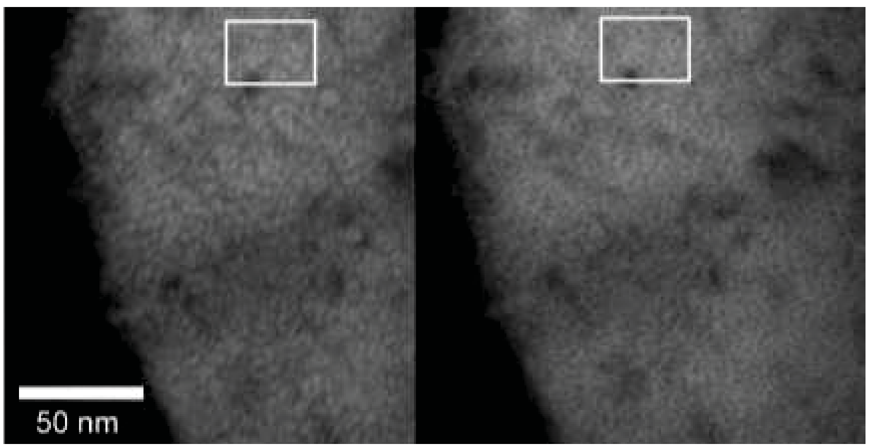

Figure 5. TEM images of under-focus (left) and over-focus (right) showing small Kr bubbles in Mo_2Zr phase irradiated with reduced energy of 250 keV Kr ions at 200 °C to 2×10^{16} ions/cm^2.

During post-irradiation TEM, it was found that there are small cracks present around the interface between the large Mo_2Zr precipitate (> 5 µm) and U-Mo-Zr alloy matrix. This is likely attributed to the volume contraction (11.3%) from radiation-induced structural change in Mo_2Zr phase that may create a tensile stress exceeding the bond strength at the interface. Interface cracks were not found for the small precipitates despite of the similar volume contraction, indicating less tensile stress built up at the precipitate and matrix interface. Perez et al found that the Mo_2Zr precipitates at the interface of U-Mo and Zr barrier layer in a fresh fuel tend to be quite small [1]. Therefore the cracks identified for the large Mo_2Zr as a result of radiation-induced structural change may not be a concern for the U-10Mo/Zr/Al-6061 monolithic fuel plate as long as the fuel fabrication process does not introduce large Mo_2Zr precipitates.

3.2 Thermal stability of gas bubble superlattice

The temperature vs. time curve for the TEM in-situ heating experiment for an irradiated U-10Mo FIB-TEM sample is shown in Figure 6. During the heating experiment, it requires frequent Z-height adjustment and correction for tilt and thermal drift to maintain the right imaging condition for GBS. Figure 7 shows the TEM bright field images of GBS at various temperatures from the same sample area. It shows no significant degradation on the superlattice structure for GBS. The GBS images accquired at room temperature before and after the in-situ heating experiment are shown in Figure 8. They demonstrate the high thermal stability of the GBS. This is not a total surprise since GBS was developed in the U-Mo fuel under very aggressive fission fragment bombardement to very high atomic displacement damage while in the reactor. The temperature-transformation-time (TTT) diagram for U-Mo indicates that for U-10Mo it may take more than 5 hours to decompose its γ-phase at 500°C [5]. Once passing 580°C, U-10Mo will be stable in its high temperature γ-phase (bcc). It is believed that GBS will collapse if γ-phase is decomposed.

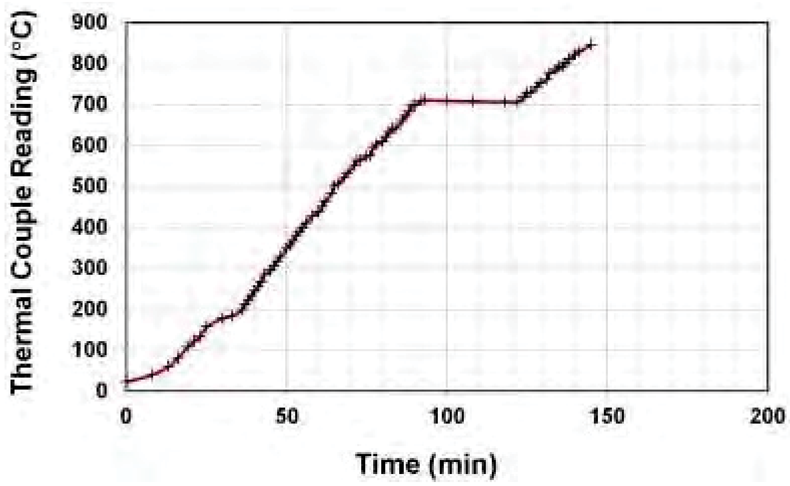

Figure 6. TC reading vs. time for TEM ins-itu heating test for an irradiated U-10Mo sample.

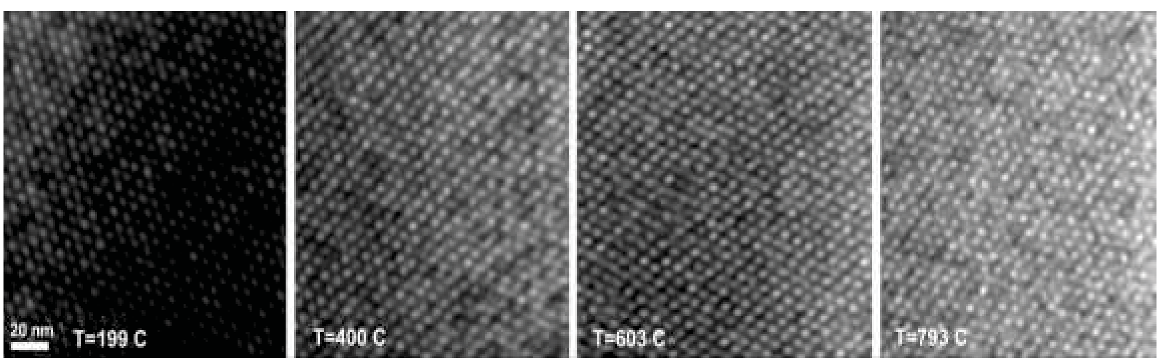

Figure 7. TEM bright field images of GBS at zone [110] at various temperatures.

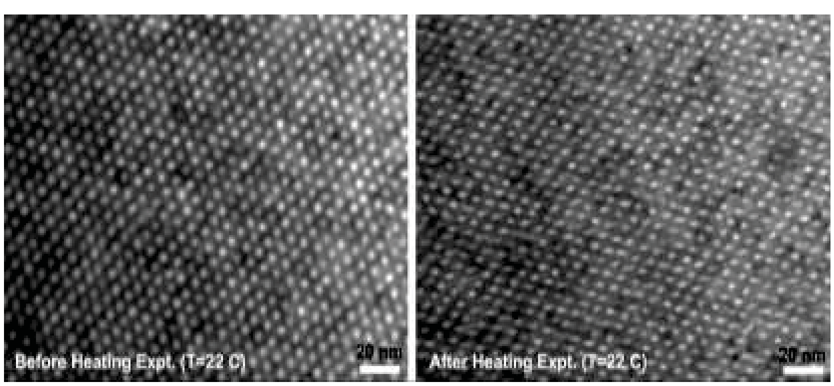

Figure 8. GBS images at room temperature before and after TEM in-situ heating experiment.

As a general concern for the in-situ TEM experiments, the small sample dimension plus the technical difficulty in calibrating the FIB-TEM spcimen temperature for the TEM heating holder, the observation from this work needs to be verified by the furnace annealing experiment of a bulk irradiated fuel sample followed by TEM characterization. This work has been planned and the results will be provided in the future publication or conference. To better understand the correlation between the γ-pahse stability on GBS stability in U-Mo fuel, it is desired to conduct heating experiment for the irradiated U-7Mo fuel instead of the U-10Mo fuel since the former may start the phase transformation in about 1 hour at 525°C which is much sooner than that of U-10Mo fuel.

4. Conclusions

The Mo_2Zr phase developed at U-10Mo/Zr interface from fuel fabrication has an $MgCu_2$ type large and complex cubic structure. Under Kr ion irradiation at 200 °C temperature to fluence of 2×10^{16} ions/cm^2, this phase changes its structure to a much smaller bcc cubic associated with a volume contraction of 11.3%. The irradiated defect structure mainly consists of dislocation tangles and network. Ignoring the radiation-induced structural change, the Mo_2Zr phase shows exceptional radiation tolerance on suppressing bubble formation and maintaining crystalline structure up to high dose of ~ 145 dpa. The preliminary result from TEM in-situ hjeating of an irradiated U-10Mo demosntrated the high thermal stability of gas bubble superlattice.

Acknowledgments

Acknowledgment is given to Glenn Moore for alloy fabrication and Francine Rice for help on TEM heating experiment at Idaho National Laboratory, and Pete M. Baldo for ion irradiation at Argonne National Laboratory. The in-situ ion irradiation and electron microscopy was accomplished at the Electron Microscopy Center for Materials Research at Argonne National Laboratory, a U.S. Department of Energy Office of Science Laboratory operated under Contract No. DE-AC02-06CH11357 by UChicago Argonne, LLC. This work was supported by the U.S. Department of Energy, Office of Nuclear Materials Threat Reduction (NA-212), National Nuclear Security Administration to the RERTR program, under DOE-NE Idaho Operations Office Contract DE-AC07-05ID14517. Accordingly, the U.S. Government retains a nonexclusive, royalty-free license to publish or reproduce the published form of this contribution, or allow others to do so, for U.S. Government purposes.

References

[1] E. Perez, B. Yao, D.D. Keiser Jr., Y.H. Sohn, J. Nucl. Mater. 402 (2010) 8-14.

[2] J. Gan, D.D. Keiser, B.D. Miller, M.A. Kirk, J. Rest, T.R. Allen, D.M. Wachs, J. Nucl. Mater 407 (2010) 48-54.

[3] J. Gan, D.D. Keiser Jr., B.D. Miller, D.M. Wachs, T.R. Allen, M. Kirk, J. Rest, J. Nucl. Mater. 411 (2011) 174-180.

[4] K. Huang, Y. Park, D.D. Keiser Jr., and Y.H. Sohn, “Interdiffusion Between Zr Diffusion Barrier and U-Mo Alloy”, Journal of Phase Equilibria and Diffusion, Vol. 33. No. 6 (2012) 443.

[5] C.A.W. Peterson, W.J. Steele, S.L. DiGiallonardo, “Isothermal Transformation Study of Some Uranium-Base Alloys”, Report: UCRL-7824, Metals, Ceramics, and Materials, UC-25, TID-4500 (34th Ed.), Lawrence Radiation Laboratory, Livermore, California, August, 1964.

[6] ASM Alloy Phase Diagrams Center, P. Villars, editor-in-chief; H. Okamoto and K. Cenzual, section editors; http://www1.asminternational.org/AsmEnterprise/APD, ASM International, Materials Park, OH, USA, 2006-2014.
[7] Ban, Z., Trojko, R., Blazina, Z., "High temperature equilibria in the Zr_{1-x} Hf_x M_2, Zr_{1-x} Ti_x M_2 and Hf_{1-x} Ti_x M_2 (M= Mo or W) systems", J. Less-Common Met. 83, 175 (1982).
[8] Blazina Z., Trojko R., Ban Z., "METAL-METALLOID EXCHANGE IN THE $Zr_{1-x}M_xMo_2$ (M = Ge, Si, Al) SYSTEM". J. Less-Common Met. 97, 91 (1984).
[9] Osten Rapp, J. Less-Common Met., 21 (1970) 27-44.
[10] J.F. Ziegler, J.P. Biersack, and U. Littmark, The Stopping and Range of Ions in Solid, Pergamon Press, New York, 1996.
[11] P. Stadelmann, http://cimewww.epfl.ch/people/stadelmann/jemsWebSite/jems.html.